Carbon and hydrogen stable isotope fractionation of sulfamethoxazole during anaerobic transformation catalyzed by *Desulfovibrio vulgaris* Hildenborough

Wei-Ying Ouyang[a,b], Steffen Kümmel[a], Lorenz Adrian[b,c], Yong-Guan Zhu[d], Hans H. Richnow[a]*

[a]Helmholtz Centre for Environmental Research – UFZ, Isotope Biogeochemistry, Leipzig, Germany

[b]Chair of Geobiotechnology, Technische Universität Berlin, Berlin, Germany

[c]Helmholtz Centre for Environmental Research – UFZ, Environmental Biotechnology, Leipzig, Germany

[d]Key Lab of Urban Environment and Health, Institute of Urban Environment, Chinese Academy of Sciences, Xiamen, China

[e]Isodetect GmbH, Leipzig, Germany

*To whom correspondence should be addressed: Hans H. Richnow, Helmholtz Centre for Environmental Research – UFZ, Isotope Biogeochemistry, Permoserstraße 15, 04318 Leipzig, Germany, E-Mail: hans.richnow@ufz.de

Keywords: Antibiotic, sulfamethoxazole, anaerobic transformation, compound-specific stable isotope analysis (CSIA), *Desulfovibrio vulgaris* Hildenborough

Abstract

The fate of antibiotics in aquatic environments is of high concern and approaches are needed to assess the transformation of antibiotics in wastewater treatment plants. Here we used the model organism *Desulfovibrio vulgaris* Hildenborough to analyze compound specific isotope fractionation associated with anaerobic transformation of the antibiotic sulfamethoxazole (SMX). The results show that the rearrangement of the isoxazole ring in SMX is leading to significant carbon and hydrogen isotopic fractionation (ε_C = -5.8±0.7‰, ε_H = -33.8±9.2‰) during anaerobic transformation. The observed carbon isotopic fractionation is significantly higher than the values reported for aerobic degradation (ε_C = -0.6±0.1‰) or abiotic reactions (ε_C = -0.8 to -4.8‰ for photolysis, ε_C = -0.8 to -2.2‰ for advanced oxidation). This indicates that carbon isotope fractionation can be used as a parameter to differentiate reaction mechanisms of SMX transformation. The corresponding apparent kinetic isotope effect ($AKIE_C$) for anaerobic transformation of SMX was 1.029±0.003, suggesting that the mechanism for anaerobic transformation is distinct from hydroxylation and oxidation mechanisms reported for microbial aerobic degradation ($AKIE_C$=1.006±0.001) and photolysis ($AKIE_C$=1.021±0.001~1.031±0.004). In addition, dual-element (C-H) isotope analysis of SMX was performed in the present study, which was achieved by utilizing gas chromatography (GC) as the separation method instead of routine liquid chromatography. This dual-element isotope analysis resulted in a Λ value of 5±3. Overall, compound specific isotope analysis can be a feasible tool to monitor the mitigation of SMX in wastewater treatment plants.

1. Introduction

Antibiotic residues have been detected in aquatic and soil environments posing risks on ecosystems and human health (Hu et al., 2010; Kümmerer, 2009; Xu et al., 2007). Recent reviews on the appearance for antibiotic in the environment addressed monitoring need for a better understanding of the soures and fate of anitbiotics in the environent, particulatly sulfonamides (Sousa et al., 2018) (Carvalho and Santos, 2016). Concentrations of antibiotic residues in the waterbody are usually far below the reported minimal inhibitory

concentrations (MICs) and acute effects on microbial populations are unlikely in most cases. Yet, it has been reported that even these low antibiotic residue concentrations can promote the development and distribution of antibiotic resistance genes (Baquero et al., 2008; Martínez, 2008). The major input routes of antibiotics into the environment originate from wastewater of private households, hospitals and animal husbandry (Karthikeyan and Meyer, 2006; Zhou et al., 2013). Concerning the latter, the bacteriostatic sulfamethoxazole (SMX; $C_{10}H_{11}N_3O_3S$) is one of the most widely and frequently used antibiotics in animal farming. Currently SMX represents one of the persistent antibiotics in waste water all over the world (Göbel et al., 2007; Hruska and Franek, 2012; Zhang and Li, 2011).

Microbial degradation contributes to the attenuation of SMX in water environments as a key route under oxic and anoxic conditions. The current knowledge on microbial degradation of SMX and the major degradation pathways have been recently reviewed (Chen and Xie, 2018; Wang and Wang, 2018). *Ipso*-hydroxylation was reported as a typical activation step for aerobic degradation of SMX by *Microbacterium* sp. strain BR1, with sulfite, 3-amino-5-methylisoxazole (3A5MI) and benzoquinone-imine (further transformed to 4-aminophenol) as products (Ricken et al., 2013; Ricken et al., 2015). The cleavage of the N-C or the S-N bond of SMX by aerobic bacteria could lead to the formation of 4-amino-N-hydrobenzensulfonamide and sulfanilamide as shown for *Pseudomonas* sp. (Jiang et al., 2014). In addition, photolysis and advanced oxidation also triggers the decrease of SMX concentrations in wastewater treatment plants (Hu et al., 2007; Ryan et al., 2011). Photolysis targets all the connecting covalent bonds between the two major moieties of SMX and generates sulfanilic acid, 3A5MI and SMX tautomers as most frequently detected products (Boreen et al., 2004; Periša et al., 2013; Trovó et al., 2009). The prevalent product 3A5MI is detected during both aerobic degradation and photolysis after the cleavage of the S-N bond. Distinct pathways were reported during anaerobic transformation of SMX by strain *Desulfovibrio vulgaris* Hildenborough (Ouyang et al., 2021). Two products were observed during anaerobic transformation of SMX showing reductive cleavage and rearrangement of the isoxazole moiety (Ouyang et al., 2021). These two transformation products were also frequently detected under other anoxic conditions

(e.g. iron-reducing condition) and in engineered systems (e.g. sulfate-reducing bioreactors) together with secondary products (Jia et al., 2017; Mohatt et al., 2011), indicating the extensive existence of the reductive cleavage and rearrangement mechanisms during anaerobic transformation of SMX. The detection of transformation products in complex environments is obstructed by unknown products and secondary transformations. Therefore, a better pathway indicator is needed to monitor the attenuation of SMX in aquatic environments, especially in wastewater treatment plants.

Compound-specific stable isotope analysis (CSIA) is a powerful and robust method to identify contaminant transformation and to estimate rates and extents of transformation (Hunkeler et al., 2008) as well as to trace *in situ* processes over time or spatially. Moreover, CSIA also has been successfully applied to characterize enzymatic reaction mechanisms (Elsner, 2010).

CSIA is based on the principle that transformation reactions proceed via formation or cleavage of bonds leading to an isotope fractionation. Kinetic isotope effects (KIEs) during these bond changes are typically caused by the preferred reaction of the lighter isotopes (e.g., ^{12}C) compared to the heavier ones (e.g., ^{13}C) because of different activation energies. Hence, heavier isotopes are usually enriched in the residual fraction of the reactant and depleted in the product fraction (Elsner et al., 2005). The extent of this isotopic change can be quantified by the Rayleigh equation and is expressed as the isotopic fractionation factor (ε). Pronounced isotopic fractionation was observed in selected enzymatic reactions and abiotic transformation (e.g. photolysis) (Liu et al., 2019; Willach et al., 2018). Differences between aerobic and anaerobic transformation have also been identified by CSIA for many compounds including hydrocarbons/BTEX (Kümmel et al., 2016; Vogt et al., 2008), chlorobenzenes (Griebler et al., 2004) and chlordecone (Chevallier et al., 2018), as the activation steps can cause specific isotope fractionation patterns and are characteristic for transformation reactions. A recent example for the application of CSIA concerning the transformation of a micropollutant was demonstrated by Knossow and colleagues (Knossow et al., 2020). They investigated the transformation of bromoxynil and observed a much larger nitrogen isotope fractionation during aerobic degradation compared to anaerobic transformation of bromoxynil. The isotope features

achieved from laboratory model cultures with known transformation pathways can be applied in field studies to characterize the *in situ* biodegradation, and hence natural attenuation (Zwank et al., 2005).

However, isotope fractionation in biological systems can be influenced by cellular mass transfer, as cross-membrane transfer as rate-limiting step prior to bond cleavage can mask the real extent of isotope effects in the reaction (Renpenning et al., 2015; Thullner et al., 2013). In order to overcome these masking effects, multi-element isotope fractionation concepts (e.g. C, H) were developed relying on lambda (Λ) values expressing the slope of changing hydrogen and carbon isotope signatures during biodegradation (Kuder et al., 2005; Vogt et al., 2016; Zwank et al., 2005). Previously, a method for carbon isotope analysis of SMX was established on HPLC-IRMS (Kujawinski et al., 2012). SMX is a polar compound with a melting point of 169°C and a high boiling point of 482°C, and SMX has a high Henry coefficient (6.4×10^{-13} atm-m^3/mol) so that HPLC is the routine method for detection. However, the HPLC-IRMS method excluded measurements of other elements like H, N and S (Kujawinski et al., 2012). Hence, only carbon isotope fractionation of SMX by microbial aerobic degradation, photolysis and oxidation was investigated by HPLC-IRMS, showing low to moderate carbon isotope effects (Birkigt et al., 2015; Willach et al., 2017; Willach et al., 2018). To our best knowledge, no data on isotope fractionation for the anaerobic transformation of SMX are available. No methods for ^{2}H analysis were available and therefore, two-dimensional isotope fractionation of SMX during transformation process remains unexplored.

The objective of this study was to develop a method for dual-element (C-H) isotope analysis of SMX on GC-IRMS, and to use the established CSIA method to evaluate the anaerobic transformation of SMX by the model organism *Desulfovibrio vulgaris* Hildenborough. For the first time we tested the feasibility of dual-element (C-H) isotope analysis of SMX. In addition, we also compared the isotope features of SMX during anaerobic transformation with that of other typical processes may occur in wastewater treatment plants, showing the potential of CSIA in assessing the attenuation of antibiotics in wastewater treatment systems.

2. Materials and Methods

2.1 Chemicals

Sulfamethoxazole (4-amino-N-(5-methyl-1,2-oxazol-3-yl)benzenesulfonamide) was purchased from Sigma-Aldrich at analytical quality. Methanol and formic acid used for UPLC mobile phases were of HPLC-grade.

2.2 Cultivation of *Desulfovibrio vulgaris* Hildenborough and detection of SMX transformation

Desulfovibrio vulgaris Hildenborough was obtained from the DSMZ (strain DSMZ 644) and cultivated as described previously using 21 mM K_2SO_4 as electron acceptor and 53.4 mM sodium lactate as electron donor and carbon source (Ouyang et al., 2021). Batch cultures were established by inoculating medium spiked with 100 µM SMX with 3% (v/v) of a pre-grown subculture. The cultures were incubated at 30°C in the dark without shaking. No-cell controls (NCC) were set up in parallel. Concertation were monitored by HPLC as described before (Ouyang et al., 2021). For details see (SI Concentration analysis).

2.3 Extraction of SMX from culture liquid

For the extraction of SMX concentrations to meet the detection limit of the GC-IRMS, SMX was extracted from cultures via solid phase extraction (SPE) and concentrated in acetone for analysis. The SPE cartridge (Waters HLB OASIS 6cc/500 mg) contained a universal hydrophilic–lipophilic balanced, polymeric reversed-phase sorbent often used for pharmaceutical analysis. The concentrated samples were stored at -20°C for subsequent UPLC-DAD analysis for concertation and the GC-IRMS measurement. More details can be for SI section.

2.4 GC-mass spectrometry (MS)

An Agilent 7890 series GC (Agilent Technologies, USA) equipped with a 5975C mass spectrometer (Agilent Technologies, USA) and a CombiPAL autosampler (CTC Analytics AG, Switzerland) was used

for SMX and metabolite analysis. Analytical details for the optimization can be found in the SI section GC-MS Analysis.

2.5 Analysis of carbon and hydrogen stable isotope ratios of SMX by GC-IRMS and elemental analysis (EA)-IRMS

Compound-specific stable carbon and hydrogen isotope analysis of SMX was performed on a Thermo Scientific MAT 253 isotope-ratio mass spectrometer (IRMS; Thermo Fisher, Germany) interfaced with an Agilent 7890 A GC system (Agilent Technologies, USA) via a GC-IsoLink and a ConFlo IV interface (Thermo Fisher, Germany). Samples were separated on the same Zebron ZB-1 column and using the same temperature program as described above for GC-MS analysis. Samples were injected into the GC system via split/splitless injector. Injection volumes were 1-5 µL adapting to SMX concentrations in samples.

Bulk stable carbon and hydrogen isotope analysis was performed using an EuroEA3000 elemental analyzer (EA, HEKAtech) connected to a Thermo Scientific MAT 253 IRMS (Thermo Fisher, Germany) interfaced via a ConFlo IV(Thermo Fisher, Germany) as described previously (Gilevska et al., 2015).

Isotope ratios are reported in delta notation ($\delta^{13}C$ or $\delta^{2}H$) based on equation (1)

$$\delta^{13}C \text{ or } \delta^{2}H = \frac{R_{sample}}{R_{standard}} - 1 \quad (1)$$

R_{sample} and $R_{standard}$ are the ratios of $^{13}C/^{12}C$ or $^{2}H/^{1}H$ of the sample or the international standard, respectively. The international standard for carbon isotopes is Vienna Dee Belemnite (VPDB) and the one for hydrogen isotopes is Vienna Standard Mean Ocean Water (VSMOW). The values are reported in delta notations (Brand and Coplen, 2012)

The linearized Rayleigh equation (Mariotti et al., 1981) was used to express the quantitative relationship between isotopic composition and degree of degradation.

$$\ln \frac{\delta_t + 1}{\delta_0 + 1} = \varepsilon \times \ln \frac{C_t}{C_0} \quad (2)$$

144 δ_t and δ_0 are the isotope ratios at time point t and at the beginning of the experiment; c_t and c_0 are the
145 corresponding concentrations of SMX at time point t and the at the start of the experiment. ε is the isotopic
146 fractionation describing the relationship between the change of isotope ratios and degradation-induced
147 decrease in concentrations.

148 The lambda value Λ was used for dual isotope (C-H) analysis. Here, hydrogen versus carbon isotope
149 signatures are correlated to obtain Λ by plotting and the $\frac{\delta^2 H_{bulk}}{\delta^{13} C_{bulk}}$ or $\frac{\Delta\delta^2\mathrm{H}}{\Delta\delta^{13}\mathrm{C}}$ normalized values to derive the
150 slope of linear regression according to equation (3).

151 $$\Lambda_{\mathrm{bulk}}^{\mathrm{H/C}} = \frac{\Delta\delta^2\mathrm{H_{bulk}}}{\Delta\delta^{13}\mathrm{C_{bulk}}} \approxeq \frac{\delta^2 H_{bulk}}{\delta^{13} C_{bulk}} \quad (3)$$

152 The uncertainties of the isotopic fractionation and the $\Lambda_{\mathrm{bulk}}^{\mathrm{H/C}}$ value were given as 95% confidence interval
153 (CI). Qualities of the isotopic fractionation and the $\Lambda_{\mathrm{bulk}}^{\mathrm{H/C}}$ value were evaluated by the correlation parameter
154 of the linear regression (R^2), the respective isotope fractionation was regarded as significant if R^2 was higher
155 than 0.8.

156 The apparent kinetic isotope effect (AKIE) values normalize the bulk isotope effect to the isotope effect of
157 the bond cleavage reaction to compare observable bulk stable isotope fractionation of various
158 transformation pathways (Elsner et al., 2005). The isotopic fractionation (ε) was normalized to the number
159 of atoms located in reactive positions for bond changes. Therefore, the bulk isotope ratios (δ_{bulk}) were
160 converted to the isotope ratios of reactive positions ($\delta_{\mathrm{reactive\ position}}$) using equation (4), and the isotopic
161 fractionation of the reactive position ($\varepsilon_{\mathrm{reactive\ position}}$) was calculated based on the corrected $\delta_{\mathrm{reactive\ position}}$
162 and linearized Rayleigh equation.

163 $$\delta_{\mathrm{reactive\ position}} = \delta_{\mathrm{bulk}} \times \frac{\mathrm{n}}{\mathrm{x}} \quad (4)$$

164 Here, n is the total number of atoms for one element and x is the number of atoms at the reactive
165 positions.

Apart from the correction for isotopic fractionation of the reactive position ($\varepsilon_{\text{reactive position}}$), the calculation of AKIE values was also based on a second correction due to the location of non-discriminable atoms of one element at the reactive positions in equation (5).

$$\text{AKIE}=\frac{1}{1+z\times\varepsilon_{\text{reactive position}}/1000} \quad (5)$$

Here, z is the number of atoms in indistinguishable reactive positions which result in intramolecular competition. The uncertainties of AKIE values were calculated by error propagation in equation (6).

$$error\ of\ AKIE=\left|\frac{\partial AKIE}{\partial \varepsilon_{reactive\ position}}\right|\times error\ of\ \varepsilon_{reactive\ position} \quad (6)$$

3. Results and discussion

3.1 Method development for GC-MS and GC-IRMS

We developed and optimized a method for carbon and hydrogen isotope analysis on GC-IRMS. Previously the carbon isotope composition was analyzed by HPLC-IRMS (Birkigt et al., 2015) which is neither amenable for ^{2}H isotope analysis nor for ^{15}N or ^{34}S isotope ratio measurements. In the first step we established a separation method for SMX on GC without additional derivatization steps to overcome the drawbacks of HPLC, as derivatization can cause bias in isotope ratios. The injector temperature of GC was tested from 180°C to 260°C to monitor the vaporization and avoid decomposition of SMX. The SMX peak and product peaks were identified by comparison with the NIST library identification confidence above 90%. The peak area of the SMX peak did not vary significantly when the injector temperature was varied (**Error! Reference source not found.**). At a temperature of 180°C, the SMX peak showed tailing and the ion signals were not reproducible, resulting in high standard deviation (**Figure S2**). The SMX peak shape improved at temperatures above 200°C but by-products started to form. The three by-products from the thermal decomposition of SMX were tentatively identified by GC-MS: the most abundant by-product had fragment masses very similar to sulfanilamide which can be generated when the N-C bond

between the sulfonamide group and the isoxazole moiety in SMX is cleaved; aniline and 4-aminothiophenol were less abundant by-products compared to sulfanilamide (**Figure S3**, **Table S1**). The combined area counts of the by-products related to the sum of the area counts of SMX and by-products together ranged up to 5.5% at different injector temperatures. The proportion of by-product area counts increased with increasing injector temperatures. At temperatures above 240°C, the amount of by-products decreased, suggesting that the primary by-products undergo further decomposition (**Figure S2**). The the lowest decomposition of SMX was observed at 200°C (2.5%) (**Figure S2**). Therefore, 200°C was selected as the optimal injector temperature for detection of SMX by GC. With the developed temperature program for separation and the selected injector temperature, we tested SMX standards with different concentrations from 1 mM to 125 mM by GC-MS using 1 µL injection. No signal was detected at 1 mM, but a linear response was observed between 5 and 50 mM. At concentrations above 50 mM the linear correlation was lost (**Figure 1a**). The losses of SMX at higher concentrations could be due to incomplete evaporation in the injector, formation of by-products and/or saturation of the detector. We detected more by-products of up to 11% at higher SMX concentrations (**Figure 1b**) but these amounts were quantitatively not amounting to the amount of SMX missing from the detection at higher concentrations. For our application it was important to observe that SMX decomposition was significantly reduced at SMX concentrations between 5 and 50 mM.

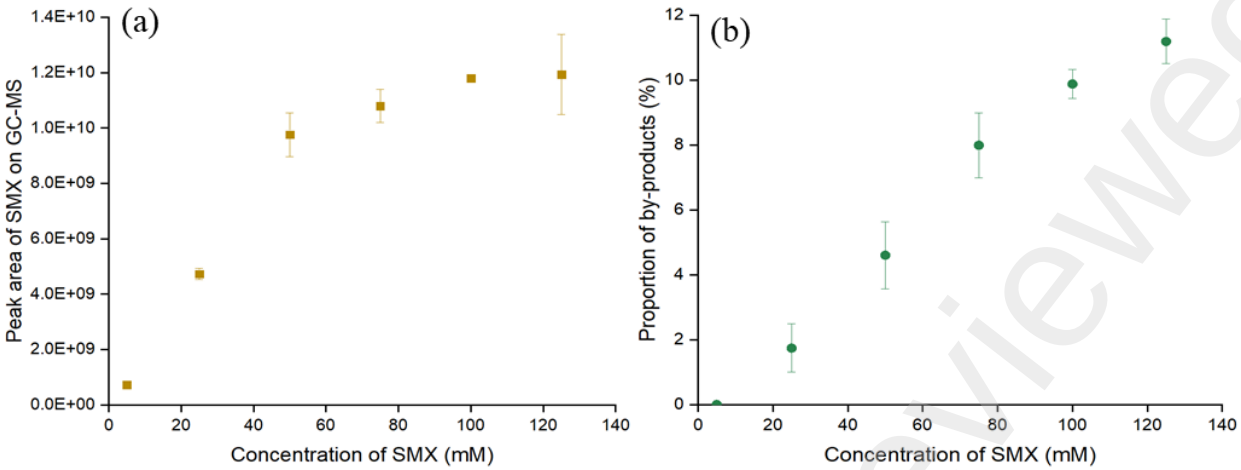

205

206 **Figure 1.** Signal response of SMX and proportion of by-products at different concentrations of SMX on GC-MS.
207 **a)** Peak areas of SMX ions (yellow blocks) on GC-MS at different concentrations of SMX; **b)** proportions of by-
208 products (green dots) in total signals at different concentrations of SMX.

209 ## 3.2 Dependency of carbon and hydrogen isotope values on concentration

210 The dependency of isotope composition on the concentrations of SMX was determined to select the
211 dynamic range of concentrations (linear range) where the isotope composition can be reproducibly
212 determined. Therefore, the peak areas of SMX are plotted against the isotope composition (**Figure**).
213 Carbon and hydrogen isotope signatures ($\delta^{13}C$ and $\delta^{2}H$) of SMX were measured by GC-IRMS with the
214 optimum GC operation parameters described above. A series of SMX standards (1 mM to 125 mM) were
215 injected with different volumes (1 µL, 3 µL and 5 µL) to test the stable ranges of carbon and hydrogen
216 isotope signatures, and the hydrogen data was adjusted based on the H_3^+ factor. The experiments showed
217 that when the injected SMX surpassed certain amounts, both carbon and hydrogen isotope ratios reached
218 a stable range with reproducible results. This indicates that within a stable range isotope ratios are
219 independent of bulk concentrations of SMX. When the peak area of SMX was above 5 Vs, the carbon
220 isotope ratio $\delta^{13}C$ was consistently at -26.5 ± 0.5‰ (Figure **2**a). Larger loading amounts of SMX (>13
221 Vs) were needed to reach the determined stable range of hydrogen isotope ratios $\delta^{2}H$ (-127 ± 6‰)
222 (**Figure** b). Based on elemental analysis, the bulk ^{13}C isotope ratio of SMX was -26.3 ± 0.1‰ (**Figure** a),
223 and the bulk ^{2}H isotope ratio of SMX was -125 ± 3‰ (**Figure** 2b). Both the carbon and hydrogen isotope

ratios achieved from our developed GC-IRMS methods are in line with the bulk values directly obtained from elemental analyzer, which confirms the validity of the developed GC-IRMS method for SMX analysis. Dual isotope analysis of SMX by GC-IRMS provides more possibilities to characterize transformation processes compared with previously reported one-dimensional HPLC-IRMS (Birkigt et al., 2015) and HT-LC-IRMS methods (Kujawinski et al., 2012), which can only analyze carbon isotope ratios in sulfonamides. However, isotope data for other elements are crucial to investigate SMX transformation. For example, by screening photolysis products, Willach found that apart from carbon (Willach et al., 2018) other atoms such as N and S are also directly involved in bond cleavage for products formation, therefore, multiple element isotope analysis is essential.

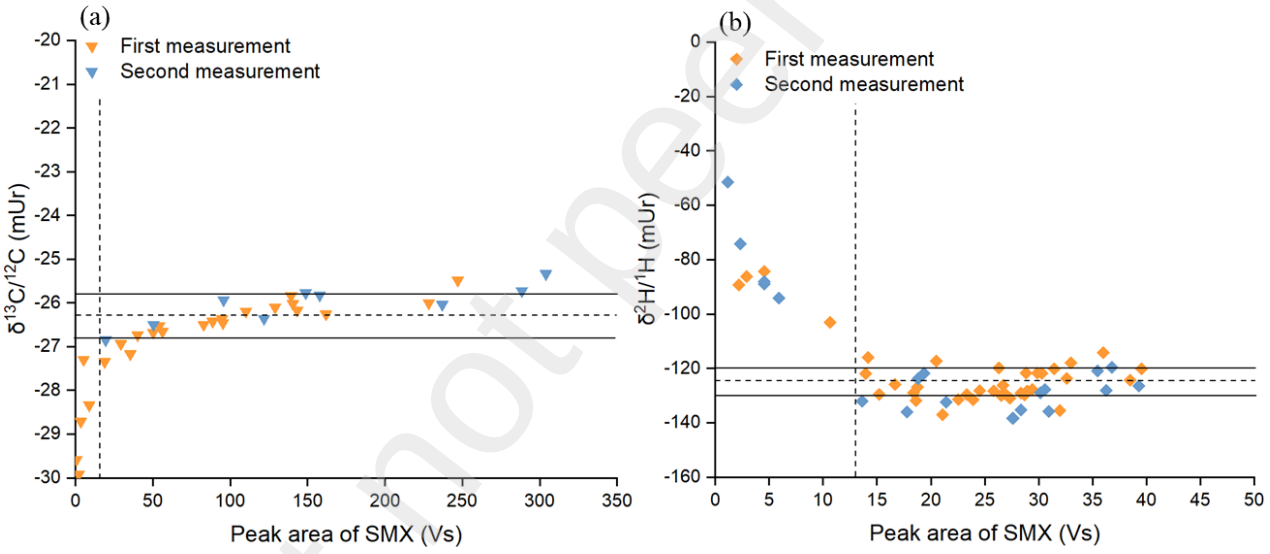

Figure 2. Carbon and hydrogen stable isotope ratios of SMX at different concentrations of SMX. **a)** Linear range of carbon isotope ratio (triangles) of SMX; **b)** linear range of hydrogen isotope ratio (diamonds) of SMX. The vertical dash lines in panels a) and b) indicate the peak area from which the data was considered to be stable. The horizontal dash lines indicate the mean value from elemental analysis and the horizontal solid lines indicate the uncertainties (95% confidence interval) of elemental analysis. Two independent measurements were performed with the same SMX standards shown in different colors.

3.3 Carbon and hydrogen stable isotope fractionation during the anaerobic transformation of SMX by *Desulfovibrio vulgaris* Hildenborough

In order to analyze ^{2}H and ^{13}C isotope fractionation of SMX during anaerobic transformation, 20 parallel cultures of *Desulfovibrio vulgaris* Hildenborough were established with 53.4 mM lactate as electron donor and carbon source, 21 mM sulfate as electron acceptor, and 100 μM SMX as the substrate. A previous study reported that *Desulfovibrio vulgaris* Hildenborough transformed SMX to two products (TP1 and TP2) stoichiometrically at a wide concentration range of SMX (Ouyang et al., 2021). The transformation occurred on the isoxazole moiety of SMX caused by reductive cleavage (TP1) or rearrangement (TP2) (**Figure 5**). In the established batch cultures for isotope fractionation analysis, almost 75% of the spiked SMX (100 μM) was transformed by *Desulfovibrio vulgaris* Hildenborough after 9 days cultivation. In order to obtain samples in which 0 to 75% of spiked SMX was transformed, batch cultures were sacrificed from day 5 to day 9, as no transformation was observed for the first 4 days.

Significant carbon and hydrogen stable isotope fractionations of SMX were observed during anaerobic transformation of SMX by *Desulfovibrio vulgaris* Hildenborough. The carbon isotope composition of SMX changed from -26.5‰ to -18.6‰ after 65% transformation of SMX at day 8 of the cultivation (**Figure S4**). The isotope fractionation could be quantified using the Rayleigh equation, yielding an isotopic fractionation (ε_C) for carbon of -5.8±0.7‰ with a good correlation as indicated by the coefficient of determination (R^2=0.98) (**Figure A**). The carbon isotope fractionations of SMX during microbial aerobic degradation, photolysis and oxidation of previous studies were also examined for comparison (**Table 1**) (Birkigt et al., 2015; Willach et al., 2017; Willach et al., 2018). The ε_C value (-5.8±0.7‰) characterizing anaerobic transformation of SMX, was much higher than that of aerobic degradation by *Microbacterium* sp. strain BR1 (-0.6±0.1‰). The activation step for anaerobic transformation by *Desulfovibrio vulgaris* is a reductive cleavage of the N-O bond (Ouyang et al., 2021) while aerobic degradation by *Microbacterium* sp. is initiated by *ipso*-hydroxylation (Ricken et al., 2013). The different mechanisms of aerobic and anaerobic transformation can be distinguished by the observed carbon isotope fractionations. In addition to the

differences in degradation mechanism, the much higher observed ε_C value for anaerobic transformation could also be attributed to a lower masking effect (Renpenning et al., 2015). Anaerobic transformation was proposed as a periplasmic process similar to the periplasmic reduction of heavy metals by cytochrome c in *Desulfovibrio* (Lovley and Phillips, 1992; Lovley et al., 1993; Ouyang et al., 2021). In contrast, for aerobic degradation Ricken et al. proposed that a cytoplasmic NADH-dependent monooxygenase catalyzes the hydroxylation of SMX (Ricken et al., 2015), may inducing stronger masking effects and thus a lower ε_C value.

The reported ε_C value for direct photolysis was also lower than the one we observed for anaerobic transformation and depended on wavelength and pH values. At pH 5 and 7.4 using artificial sunlight with a wavelength range of 300−800 nm, the ε_C values were -3.0±0.1‰ and -2.0±0.1‰, respectively (**Table 1**). However, direct photolysis with short UV wavelength (254 nm) caused trivial (up to 0.8±0.1‰) to no observable carbon fractionation. The wavelength between 310-600 nm, which may be relevant for sunlight at the surface at sea level, gave ε_C values of -3.9±0.1‰ and -4.8±0.1‰ depending on the pH value. At pH 3 among all photolysis products, the most abundant one has a rearranged isoxazole ring which has the same structure as detected in TP2 for anaerobic transformation, in the meantime, the observed ε_C value reached -4.8±0.1‰ approaching the carbon fractionation range induced by anaerobic transformation (-5.8±0.7‰). Therefore, we propose that the formation of TP2 is causing the large carbon isotope fractionation. In summary, the abiotic reactions (e.g. photolysis and oxidation) are not as selective as enzymatic reactions, cleavage at various positions undergoes simultaneously resulting in various degradation products. The observed ε_C values are derived from the mixture of different mechanisms and depend on the ratios of products (Willach et al., 2017). This fact can explain the varying ε_C values observed during photolysis and advanced oxidation, and relatively lower ε_C values compared with that of anaerobic transformation.

We also determined hydrogen isotope fractionation during microbial SMX transformation. During the anaerobic transformation process, the hydrogen isotope composition shifted from -148‰ at time 0 to -124‰

after 7 days of incubation when 52% of the initial SMX was transformed. The two points with the lowest SMX concentrations showing relatively large standard deviation (**Figure S4**) may introduce uncertainties for hydrogen isotope analysis. We observed that the isotopic fractionation for hydrogen (ε_H) during anaerobic transformation of SMX by *Desulfovibrio vulgaris* Hildenborough was -34±9‰ with significant correlation between SMX concentration and hydrogen isotope signatures (R^2=0.82) (**Figure**). This is the first study to report hydrogen isotope fractionation of SMX, as no hydrogen isotope data are available for SMX via HPLC-IRMS in previous studies (Birkigt et al., 2015; Willach et al., 2017; Willach et al., 2018). No hydrogen atom is directly involved in the bond cleavage according to the proposed mechanism (**Figure**), thus, the observed hydrogen isotope fractionation of SMX should be caused by a relative large secondary isotope kinetic effects (Kümmel et al., 2016). We assume that the substituted hydrogen atom at the C_4 atom (mark red in **Figure**) contributes to the change of hydrogen isotope ratios during the formation of TP2 intermediate, as the three-membered-ring in TP2 intermediate increased the available oscillation space for the hydrogen atom attached to the C_4 atom and this delocalization is better supported by ^1H than by ^2H (Aelion et al., 2009), resulting in enrichment of deuterium in the remaining SMX.

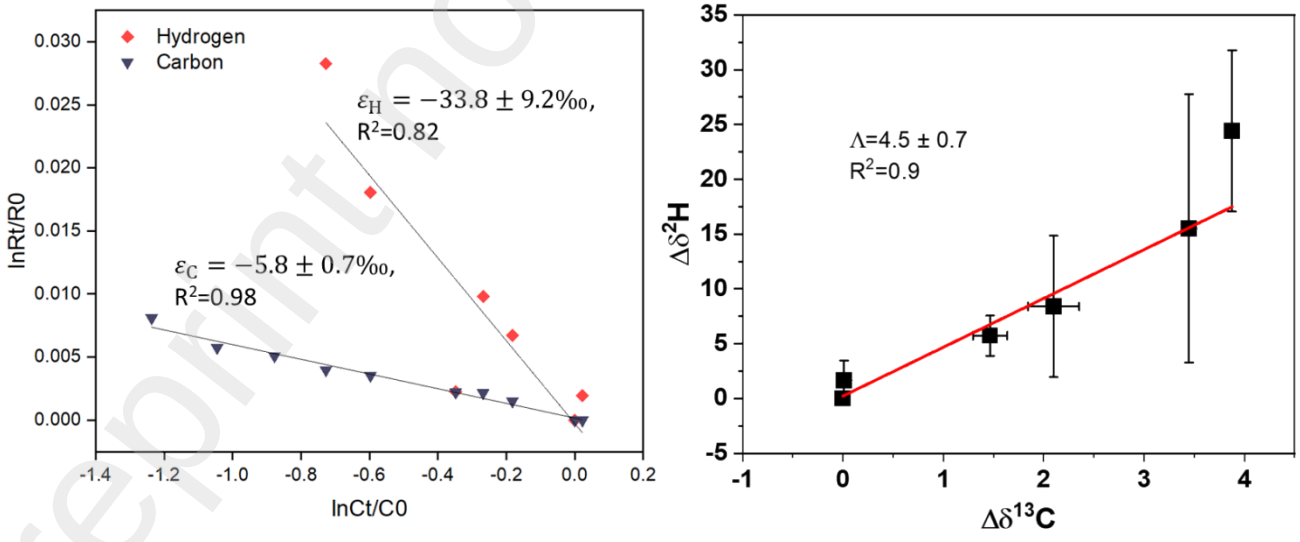

Figure 3. Rayleigh plots (A) for carbon (dark blue triangles) and hydrogen (red diamonds) and dual plot (B) for the anaerobic transformation of SMX by *Desulfovibrio vulgaris* Hildenborough. The isotopic fractionation for carbon (ε_C) and hydrogen (ε_H) were calculated based on the linearized Rayleigh equation. R^2 indicates the correlation between the change of isotope composition and the change of SMX concentration. Error bars on the dual-plots represent analytical uncertainty of each isotope system. Uncertainty of ε and Λ is calculated as 95% C.I. of the slope.

3.4 Apparent kinetic isotope effect (AKIE)

According to the previously proposed anaerobic transformation mechanism (Ouyang et al., 2021), the activation step is the reductive cleavage of the isoxazole ring moiety with subsequent electron rearrangement. Anaerobic transformation of SMX has been proposed to be initiated by nucleophilic attack onto the N atom and the common intermediate would be generated after cleavage of the N-O bond, followed by electron rearrangement along two different pathways (**Figure**). Therefore, the corresponding AKIE values for carbon and hydrogen ($AKIE_C$ and $AKIE_H$) were calculated based on the equations (7), (8) and (9) and compared with reported values from microbial aerobic degradation and chemical reactions in **Table 1**.

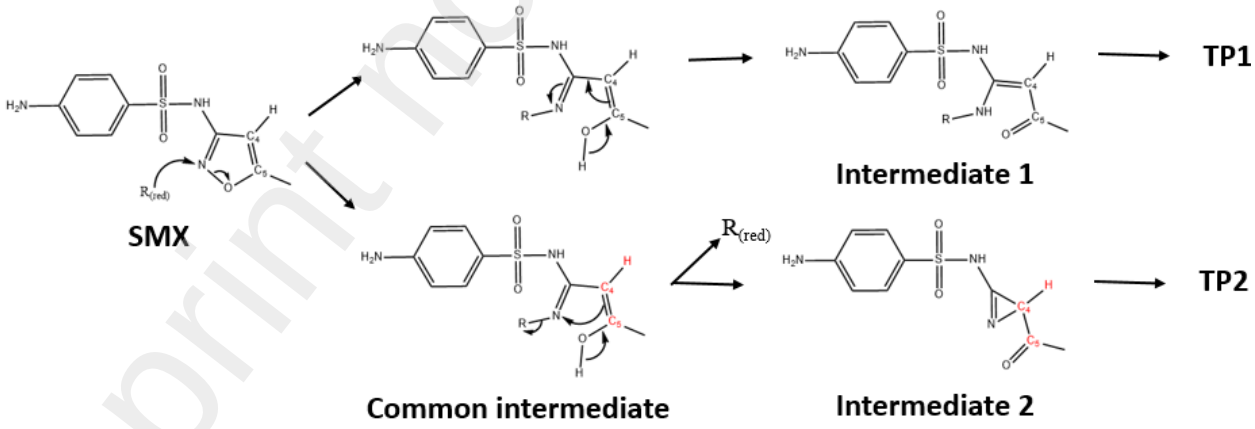

Figure 4. Initial reactions of anaerobic transformation of SMX by *Desulfovibrio vulgaris* Hildenborough activated by a reducing agent $R_{(red)}$. Elements (C_4, C_5 and H) in red represent atoms are at the reactive positions (modified from literature (Ouyang et al., 2021)).

2 out of 10 carbon atoms are at the reactive positions

$$\delta_{reactive\ position}=\delta_{bulk} \times \frac{10}{2} \quad (7)$$

And 1 out of 11 hydrogen atoms is located at the reactive position

$$\delta_{reactive\ position}=\delta_{bulk} \times \frac{11}{1} \quad (8)$$

Based on the mechanism illustrated in **Figure** , the number z is 1 for both carbon and hydrogen atoms during the formation of TP1 intermediate and TP2 intermediate.

—The $AKIE_C$ value of anaerobic transformation by *Desulfovibrio vulgaris* Hildenborough was 1.029±0.003, which is significantly different from that of aerobic degradation by *Microbacterium* sp. strain BR1 as 1.006±0.001 (**Table 1**). Hence, the $AKIE_C$ value obtained here further support that the anaerobic transformation utilizes different mechanism from that of aerobic degradation. The $AKIE_C$ value for aerobic degradation (upon *ipso*-hydroxylation) fits in the same range of aromatic ring hydroxylation of BTEX ($AKIE_C$ (benzene) =1.005±0.001, $AKIE_C$ (toluene) = 1.006±0.001) (Fischer et al., 2008; Vogt et al., 2008) and the theoretical range for epoxidation-like C=C bond cleavage ($AKIE_C$=1.00 to 1.01) (Elsner et al., 2005). $AKIE_C$ (1.029±0.003) of anaerobic transformation is close to the reported value of anaerobic biodegradation of p-cresol by sulfate reducing bacteria ($AKIE_C$=1.028) (Elsner et al., 2005; Morasch et al., 2004), and also fits in the theoretical range of oxidation of C=C bonds with permanganate via dihydroxylation (1.025-1.028) (DelMonte et al., 1997; Elsner et al., 2005). In this study, we also obtained $AKIE_H$ value for anaerobic transformation of SMX as 1.469±0.170, but there are no reported $AKIE_H$ values for SMX in literatures for comparison.

To further test the proposed transformation mechanism in **Figure** , we also tried to analyze the isotope composition of the transformation products, but peaks of TP1 and TP2 were not detected using the hydrogen isotope analysis method as the amounts of products were not sufficiently large. Only the TP1 peak was

detected under carbon isotope analysis mode and the structure of TP1 was confirmed by GC-MS. We observed that the carbon isotope ratios of TP1 kept consistent during transformation of SMX (**Figure S5**). This result indicates that the formation of TP1 did not contribute to the fractionation of SMX, which is in line with the hypothesis shown in **Figure** that only the formation of TP2 induced carbon fractionation of SMX.

351 **Table 1.** Bulk isotopic fractionation ($\varepsilon_{C\,bulk}$), AKIE and Lambda values for the aerobic degradation of SMX by *Microbacterium* sp., anaerobic

352 transformation of SMX by *Desulfovibrio vulgaris* Hildenborough and abiotic transformation of SMX including photolysis and oxidation.

Microbial and abiotic transformation of SMX	Initial concentration of SMX [µM]	ε_C_{bulk} [‰], (R^2)	AKIE C	ε_H_{bulk} [‰], (R^2)	AKIE H	ΛH/C, (R^2)	Reference
Desulfovibrio vulgaris Hildenborough	100	-5.8±0.7 (0.98)	1.029±0.003	-34±9 (0.81)	1.469±0.170	5±3 (0.77)	This study
Microbacterium sp. strain BR1	500	-0.6±0.1 (0.86)	1.006±0.001	N.D.	N.D.	N.D.	(Birkigt et al., 2015)
Direct photolysis at pH 7.4	1000	-2.0±0.1 (0.94) 300-800 nm	1.021±0.002	N.D.	N.D.	N.D.	(Birkigt et al., 2015)
Direct photolysis at pH 5	1000	-3.0±0.1 (0.95) 300-800 nm	1.031±0.004	N.D.	N.D.	N.D.	(Birkigt et al., 2015)
Direct photolysis at pH 3	790	0.8±0.1 (LP 254 nm), N.S. (MP, 200-600 nm), -4.8±0.1 (MP 310-600 nm), -1.9±0.1 (HP 220-500 nm)	N.D.	N.D.	N.D.	N.D.	(Willach et al., 2018)
Direct photolysis at pH 8	790	N.S. (LP 254 nm), N.S. (MP, 200-600 nm), -3.9±0.1 (MP	N.D.	N.D.	N.D.	N.D.	(Willach et al., 2018)

		310-600 nm), -2.2±0.2 (HP 220-500 nm)					
Oxidation at pH 3	790	-1.2±0.1 (O3), -2.2±0.1 (O3+DMSO), -0.8±0.1 (ClO2)	N.D.	N.D.	N.D.	N.D.	(Willach et al., 2017)
Oxidation at pH 8	790	N.S. (O3), N.S. (O3+DMSO), -1.3±0.1 (ClO2)	N.D.	N.D.	N.D.	N.D.	(Willach et al., 2017)

353 N.D. means not detected or not available in the related studies; N.S. means the isotope fractionation is not significant under these conditions; LP
354 represents low pressure irradiation source, MP represents medium pressure irradiation source and HP represents high pressure irradiation source,
355 respectively.

3.5 Correlation between carbon and hydrogen isotope fractionation

We further delineated the correlation between the change of carbon and hydrogen isotope ratios during anaerobic transformation of SMX by *Desulfovibrio vulgaris* Hildenborough, corresponding to a $\Lambda_{bulk}^{H/C}$ value of 5±3 (**Fig 3B**). The correlation between carbon and hydrogen isotope compositions further supports the observed hydrogen isotope fractionation during anaerobic transformation. As this is the first dual-element isotope fractionation study for SMX, there is no reported lambda value available from the literature for comparison. Nevertheless, in our study we show that dual-element analysis of SMX is feasible and could be further used to monitor attenuation of SMX in the environment without assessing product formation, which is critical for risk assessment and developing remediation solutions.

4. Conclusions

Occurrence of antibiotics in the water systems poses serious health and ecological risks. Monitoring the dissipation of residue antibiotics is crucial to evaluate the treatment efficiency of municipal wastewater treatment plants and attenuation under natural settings. In our study, we evaluated the anaerobic transformation of SMX by *Desulfovibrio vulgaris* Hildenborough by CSIA and proposed CSIA developed here as a robust tool for monitoring the fate of SMX in the aquatic environments. The key conclusions of this study could be drawn as follows:

1) The high carbon isotope fractionation during anaerobic transformation of SMX, possibly caused by the formation of rearranged product TP2 which is significantly different from the minor fractionation observed during aerobic degradation, and moderate fractionation observed during advanced oxidation and photolysis.
2) The correlation between change of carbon isotopes and change of hydrogen isotopes ($\Lambda_{bulk}^{H/C}$) was delineated during anaerobic transformation of SMX.
3) The isotope features of SMX, especially the carbon isotope, are robust parameters for monitoring the mitigation of antibiotics in wastewater treatment plants. The isotopic fractionations obtained

for aerobic degradation, anaerobic transformation, photolysis and advanced oxidation can provide reference for CSIA in field study: By measuring the isotope fractionation of SMX, someone can identify different pathways and calculate their contributions during the attenuation of SMX, besides, someone can also monitor the efficiency of each treatment unit for removal of SMX in wastewater treatment plants. Further isotope fractionation studies on sulfonamides may contribute to fill gas in process studies for better understanding of natural degradation processes (Carvalho and Santos, 2016).

Declaration of Competing Interest

The authors declare no competing financial interest.

Acknowledgements

The work was supported by a Chinese Scholarship Council grant to Weiying Ouyang No. 201504910687. Isotope ratio mass spectrometry was done at the Laboratory of Stable Isotopes (LSI) at the Helmholtz Centre for Environmental Research, which is supported by European regional development funds (EFRE—Europe Funds Saxony) and the Helmholtz Association. We thank Dr. Yaqing Liu for the constructive suggestions and discussions.

Supplementary materials

Supplementary material associated with this article can be found, in the online version

References

Aelion, C.M., Höhener, P., Hunkeler, D. and Aravena, R. (2009) Environmental isotopes in biodegradation and bioremediation, CRC Press, https://www.webofscience.com/wos/woscc/full-record/WOS:A1981MS86000007.

Baquero, F., Martínez, J.-L. and Cantón, R. 2008. Antibiotics and antibiotic resistance in water environments. Current Opinion in Biotechnology 19(3), 260-265.

Birkigt, J., Gilevska, T., Ricken, B., Richnow, H.-H., Vione, D., Corvini, P.F.-X., Nijenhuis, I. and Cichocka, D. 2015. Carbon stable isotope fractionation of sulfamethoxazole during biodegradation by *Microbacterium* sp. strain BR1 and upon direct photolysis. Environmental Science & Technology 49(10), 6029-6036.

Boreen, A.L., Arnold, W.A. and McNeill, K. 2004. Photochemical fate of sulfa drugs in the aquatic environment: sulfa drugs containing five-membered heterocyclic groups. Environmental Science & Technology 38(14), 3933-3940.

Brand, W.A. and Coplen, T.B. 2012. Stable isotope deltas: tiny, yet robust signatures in nature. Isotopes in Environmental and Health Studies 48(3), 393-409.

Carvalho, I.T. and Santos, L. 2016. Antibiotics in the aquatic environments: A review of the European scenario. Environment International 94, 736-757.

Chen, J. and Xie, S. 2018. Overview of sulfonamide biodegradation and the relevant pathways and microorganisms. Science of the Total Environment 640, 1465-1477.

Chevallier, M.L., Cooper, M., Kümmel, S., Barbance, A., Le Paslier, D., Richnow, H.H., Saaidi, P.-L. and Adrian, L. 2018. Distinct carbon isotope fractionation signatures during biotic and abiotic reductive transformation of chlordecone. Environmental Science & Technology 52(6), 3615-3624.

DelMonte, A.J., Haller, J., Houk, K., Sharpless, K.B., Singleton, D.A., Strassner, T. and Thomas, A.A. 1997. Experimental and theoretical kinetic isotope effects for asymmetric dihydroxylation. Evidence supporting a rate-limiting "(3+ 2)" cycloaddition. Journal of the American Chemical Society 119(41), 9907-9908.

Elsner, M. 2010. Stable isotope fractionation to investigate natural transformation mechanisms of organic contaminants: principles, prospects and limitations. J. Environ. Monit. 12(11), 2005-2031.

Elsner, M., Zwank, L., Hunkeler, D. and Schwarzenbach, R.P. 2005. A new concept linking observable stable isotope fractionation to transformation pathways of organic pollutants. Environmental Science & Technology 39(18), 6896-6916.

Fischer, A., Herklotz, I., Herrmann, S., Thullner, M., Weelink, S.A., Stams, A.J., Schlömann, M., Richnow, H.-H. and Vogt, C. 2008. Combined carbon and hydrogen isotope fractionation investigations for elucidating benzene biodegradation pathways. Environmental Science & Technology 42(12), 4356-4363.

Gilevska, T., Gehre, M. and Richnow, H.H. 2015. Multidimensional isotope analysis of carbon, hydrogen and oxygen as tool for identification of the origin of ibuprofen. Journal of Pharmaceutical and Biomedical Analysis 115, 410-417.

Göbel, A., McArdell, C.S., Joss, A., Siegrist, H. and Giger, W. 2007. Fate of sulfonamides, macrolides, and trimethoprim in different wastewater treatment technologies. Science of the Total Environment 372(2-3), 361-371.

Griebler, C., Adrian, L., Meckenstock, R. and Richnow, H. 2004. Stable carbon isotope fractionation during aerobic and anaerobic transformation of trichlorobenzene. FEMS Microbiology Ecology 48(3), 313-321.

Hruska, K. and Franek, M. 2012. Sulfonamides in the environment: a review and a case report. Vet. Med. 57(1), 1-35.

Hu, L., Flanders, P.M., Miller, P.L. and Strathmann, T.J. 2007. Oxidation of sulfamethoxazole and related antimicrobial agents by TiO2 photocatalysis. Water Research 41(12), 2612-2626.
Hu, X., Zhou, Q. and Luo, Y. 2010. Occurrence and source analysis of typical veterinary antibiotics in manure, soil, vegetables and groundwater from organic vegetable bases, northern China. Environmental Pollution 158(9), 2992-2998.
Hunkeler, D., Meckenstock, R.U., Sherwood Lollar, B., Schmidt, T.C., Wilson, J., Schmidt, T. and Wilson, J. 2008 A guide for assessing biodegradation and source identification of organic ground water contaminants using compound specific isotope analysis (CSIA), US EPA, Oklahoma, USA,.
Jia, Y., Khanal, S.K., Zhang, H., Chen, G.-H. and Lu, H. 2017. Sulfamethoxazole degradation in anaerobic sulfate-reducing bacteria sludge system. Water Research 119, 12-20.
Jiang, B., Li, A., Cui, D., Cai, R., Ma, F. and Wang, Y. 2014. Biodegradation and metabolic pathway of sulfamethoxazole by *Pseudomonas psychrophila* HA-4, a newly isolated cold-adapted sulfamethoxazole-degrading bacterium. Appl Microbiol Biotechnol 98(10), 4671-4681.
Karthikeyan, K. and Meyer, M.T. 2006. Occurrence of antibiotics in wastewater treatment facilities in Wisconsin, USA. Science of the Total Environment 361(1-3), 196-207.
Knossow, N., Siebner, H. and Bernstein, A. 2020. Isotope Fractionation (δ13C, δ15N) in the Microbial Degradation of Bromoxynil by Aerobic and Anaerobic Soil Enrichment Cultures. Journal of Agricultural and Food Chemistry 68(6), 1546-1554.
Kuder, T., Wilson, J.T., Kaiser, P., Kolhatkar, R., Philp, P. and Allen, J. 2005. Enrichment of stable carbon and hydrogen isotopes during anaerobic biodegradation of MTBE: microcosm and field evidence. Environmental Science & Technology 39(1), 213-220.
Kujawinski, D.M., Zhang, L., Schmidt, T.C. and Jochmann, M.A. 2012. When other separation techniques fail: compound-specific carbon isotope ratio analysis of sulfonamide containing pharmaceuticals by high-temperature-liquid chromatography-isotope ratio mass spectrometry. Analytical Chemistry 84(18), 7656-7663.
Kümmel, S., Starke, R., Chen, G., Musat, F., Richnow, H.H. and Vogt, C. 2016. Hydrogen isotope fractionation as a tool to identify aerobic and anaerobic PAH biodegradation. Environmental Science & Technology 50(6), 3091-3100.
Kümmerer, K. 2009. Antibiotics in the aquatic environment–a review–part I. Chemosphere 75(4), 417-434.
Liu, Y., Wu, L., Kohli, P., Kumar, R., Stryhanyuk, H., Nijenhuis, I., Lal, R. and Richnow, H.-H. 2019. Enantiomer and carbon isotope fractionation of α-hexachlorocyclohexane by Sphingobium indicum strain B90A and the corresponding enzymes. Environmental Science & Technology 53(15), 8715-8724.
Lovley, D.R. and Phillips, E. 1992. Reduction of uranium by *Desulfovibrio desulfuricans*. Applied and Environmental Microbiology 58(3), 850-856.
Lovley, D.R., Roden, E.E., Phillips, E. and Woodward, J. 1993. Enzymatic iron and uranium reduction by sulfate-reducing bacteria. Mar. Geol. 113(1-2), 41-53.
Mariotti, A., Germon, J.C., Hubert, P., Kaiser, P., Letolle, R., Tardieux, A. and Tardieux, P. 1981. EXPERIMENTAL-DETERMINATION OF NITROGEN KINETIC ISOTOPE FRACTIONATION - SOME PRINCIPLES - ILLUSTRATION FOR THE DENITRIFICATION AND NITRIFICATION PROCESSES. Plant and Soil 62(3), 413-430.
Martínez, J.L. 2008. Antibiotics and antibiotic resistance genes in natural environments. Science 321(5887), 365-367.
Mohatt, J.L., Hu, L., Finneran, K.T. and Strathmann, T.J. 2011. Microbially mediated abiotic transformation of the antimicrobial agent sulfamethoxazole under iron-reducing soil conditions. Environmental Science & Technology 45(11), 4793-4801.
Morasch, B., Richnow, H.H., Vieth, A., Schink, B. and Meckenstock, R.U. 2004. Stable isotope fractionation caused by glycyl radical enzymes during bacterial degradation of aromatic compounds. Applied and Environmental Microbiology 70(5), 2935-2940.

Ouyang, W.-Y., Birkigt, J., Richnow, H.H. and Adrian, L. 2021. Anaerobic Transformation and Detoxification of Sulfamethoxazole by Sulfate-Reducing Enrichments and *Desulfovibrio vulgaris*. Environmental Science & Technology 55(1), 271-282.

Periša, M., Babić, S., Škorić, I., Frömel, T. and Knepper, T.P. 2013. Photodegradation of sulfonamides and their N 4-acetylated metabolites in water by simulated sunlight irradiation: kinetics and identification of photoproducts. Environmental Science and Pollution Research 20(12), 8934-8946.

Renpenning, J., Rapp, I. and Nijenhuis, I. 2015. Substrate hydrophobicity and cell composition influence the extent of rate limitation and masking of isotope fractionation during microbial reductive dehalogenation of chlorinated ethenes. Environmental Science & Technology 49(7), 4293-4301.

Ricken, B., Corvini, P.F., Cichocka, D., Parisi, M., Lenz, M., Wyss, D., Martínez-Lavanchy, P.M., Müller, J.A., Shahgaldian, P. and Tulli, L.G. 2013. Ipso-hydroxylation and subsequent fragmentation: a novel microbial strategy to eliminate sulfonamide antibiotics. Applied and Environmental Microbiology 79(18), 5550-5558.

Ricken, B., Fellmann, O., Kohler, H.P., Schaffer, A., Corvini, P.F. and Kolvenbach, B.A. 2015. Degradation of sulfonamide antibiotics by Microbacterium sp. strain BR1 - elucidating the downstream pathway. N. Biotechnol. 32(6), 710-715.

Ryan, C.C., Tan, D.T. and Arnold, W.A. 2011. Direct and indirect photolysis of sulfamethoxazole and trimethoprim in wastewater treatment plant effluent. Water Research 45(3), 1280-1286.

Sousa, J.C.G., Ribeiro, A.R., Barbosa, M.O., Pereira, M.F.R. and Silva, A.M.T. 2018. A review on environmental monitoring of water organic pollutants identified by EU guidelines. Journal of Hazardous Materials 344, 146-162.

Thullner, M., Fischer, A., Richnow, H.-H. and Wick, L.Y. 2013. Influence of mass transfer on stable isotope fractionation. Applied Microbiology and Biotechnology 97(2), 441-452.

Trovó, A.G., Nogueira, R.F., Agüera, A., Sirtori, C. and Fernández-Alba, A.R. 2009. Photodegradation of sulfamethoxazole in various aqueous media: persistence, toxicity and photoproducts assessment. Chemosphere 77(10), 1292-1298.

Vogt, C., Cyrus, E., Herklotz, I., Schlosser, D., Bahr, A., Herrmann, S., Richnow, H.-H. and Fischer, A. 2008. Evaluation of toluene degradation pathways by two-dimensional stable isotope fractionation. Environmental Science & Technology 42(21), 7793-7800.

Vogt, C., Dorer, C., Musat, F. and Richnow, H.-H. 2016. Multi-element isotope fractionation concepts to characterize the biodegradation of hydrocarbons—from enzymes to the environment. Current Opinion in Biotechnology 41, 90-98.

Wang, J. and Wang, S. 2018. Microbial degradation of sulfamethoxazole in the environment. Applied Microbiology and Biotechnology 102(8), 3573-3582.

Willach, S., Lutze, H.V., Eckey, K., Löppenberg, K., Lüling, M., Terhalle, J., Wolbert, J.-B., Jochmann, M.A., Karst, U. and Schmidt, T.C. 2017. Degradation of sulfamethoxazole using ozone and chlorine dioxide-Compound-specific stable isotope analysis, transformation product analysis and mechanistic aspects. Water Research 122, 280-289.

Willach, S., Lutze, H.V., Eckey, K., Löppenberg, K., Lüling, M., Wolbert, J.-B., Kujawinski, D.M., Jochmann, M.A., Karst, U. and Schmidt, T.C. 2018. Direct photolysis of sulfamethoxazole using various irradiation sources and wavelength ranges insights from degradation product analysis and compound-specific stable ssiotope analysis. Environmental Science & Technology 52(3), 1225-1233.

Xu, W., Zhang, G., Li, X., Zou, S., Li, P., Hu, Z. and Li, J. 2007. Occurrence and elimination of antibiotics at four sewage treatment plants in the Pearl River Delta (PRD), South China. Water Research 41(19), 4526-4534.

Zhang, T. and Li, B. 2011. Occurrence, transformation, and fate of antibiotics in municipal wastewater treatment plants. Crit. Rev. Environ. Sci. Technol. 41(11), 951-998.

Zhou, L.-J., Ying, G.-G., Liu, S., Zhang, R.-Q., Lai, H.-J., Chen, Z.-F. and Pan, C.-G. 2013. Excretion masses and environmental occurrence of antibiotics in typical swine and dairy cattle farms in China. Science of the Total Environment 444, 183-195.

Zwank, L., Berg, M., Elsner, M., Schmidt, T.C., Schwarzenbach, R.P. and Haderlein, S.B. 2005. New evaluation scheme for two-dimensional isotope analysis to decipher biodegradation processes: Application to groundwater contamination by MTBE. Environmental Science & Technology 39(4), 1018-1029.